INTERNATIONAL JOURNAL OF INTEGRATED ENGINEERING VOL. 12 NO. 3 (2020) 151-160

© Universiti Tun Hussein Onn Malaysia Publisher's Office

IJIE

Journal homepage: http://penerbit.uthm.edu.my/ojs/index.php/ijie
ISSN : 2229-838X e-ISSN : 2600-7916

The International Journal of Integrated Engineering

Motor Vibration Analysis for the Fault Diagnosis in Non-stationary Operating Conditions

Jang-Wook Hur, Tanvir Alam Shifat*

Kumoh National Institute of Technology, 61 Daehak-ro, Gumi-si, 39177, Republic of Korea

*Corresponding Author

DOI: https://doi.org/10.30880/ijie.2020.12.03.019
Received 18 December 2019; Accepted 14 January 2020; Available online 27 February 2020

Abstract: The reliability and performance of a system with minimum life-cycle cost have become quite prominent in engineering systems. With increasing industrial applications, machines are operating in intricate conditions with higher uncertainty, causing greater vulnerability of system failure. This paper reports fault-related information of Brushless DC Motor (BLDC motor) in non-stationary operating conditions and presents several analyses to diagnose the faults. Fault diagnosis is the most crucial and important part of system prognostics which helps to increase the remaining useful life (RUL) and prevent catastrophic failures. Having both electrical and mechanical characteristics present in a BLDC motor, it shows several faults in different operating conditions. These faults cause a significant change in the vibration of the Motor. This paper deals with the anomaly detection of BLDC motor in non-stationary speed conditions using vibration signal analysis as well as extraction of several Condition Indicators (CI).

Keywords: BLDC Motor, Condition Monitoring, Fault Detection, Spectral Analysis.

1. Introduction

In the past few years, BLDC motor has gained significant popularity due to its great performance, higher efficiency and better torque to current ratio. Besides not having brushes, BLDC motors also lack a mechanical commutator. The reduction in the number of components means there are fewer parts that wear out, break, need replacing, or require maintenance. Electromagnetic interference and operational noise are also less in BLDC motors as its internal components are enclosed [1].

Nomenclatures

$x(t)$ = Motor vibration signal	τ = Time parameter
X_k = Transform values in frequency domain	ω = Frequency parameter
w = Window Function	f_n = Fundamental frequency
N = Number of samples	f_s = Sampling frequency
$\bar{x}$ = Mean of vibration samples	f_{char} = Characteristic frequency

Nevertheless, like other electronic components, a BLDC motor can also fail. Particularly, overload and overheating cause some electrical faults such as conductor break or short circuit in the stator winding, an abrupt change inresistance due to insulation aging as well as some mechanical faults such as- degradation of bearings, destruction of bearing cage, rotor shaft deformation, etc. Concurring with Industry 4.0 and an exponential increase in industrial applications, condition

*Corresponding author: *tanvirshifatbd@gmail.com*

monitoring and diagnosis have become a major concern to retain the system healthy [2, 3]. Diagnosing the intermittent failures that can lead to catastrophic field failure is the primary stage of predictive maintenance. Later, using these faults related information, a maintenance scheme is designed that can provide advanced warning of failures, indicate the health state, and, overall, increase system efficiency and lifetime. The health monitoring of the BLDC motor will play an important role in the reliability of many modern engineering fields, starting from robotics and automation to marine and transportation industries where BLDC motor is a widely used component [4].

Since both electrical and mechanical characteristics are present in a BLDC motor, it shows several faults such as- conductor break or short circuit in the stator winding, aging bearing cage, broken rotor bar, eccentricity related faults etc. When a fault takes place in the motor, it will create some abrupt changes in its vibration. We can observe and distinguish these anomalies in different operating conditions through several approaches and find the State-of-Health (SOH) of the motor. Spectral analysis for the fault detection and diagnosis of rotary machinery has been a quite popular approach this far [5,6]. Many types of researches have undergone using many techniques such as Fourier Transform, Short Time Fourier Transform (STFT), Wavelet Transform (WT) etc. that allow us to inspect a signal from different domains [7,8]. Using these time-domain analyses, frequency-domain analysis, time-frequency analysis, a system's fault can be observed visually by looking at the anomalous change in the spectrum. In different domains, anomalous signal can be observed in different extents. Besides analyzing the spectrums, we can also extract several Condition Indicators (CI) of a signal that demonstrate the SOH of a system. Several CIs are measured and presented in this paper such as- in time domain: Root Mean Square (RMS), Standard Deviation (STD), Kurtosis, Skewness, Crest Factor (CF) and in frequency domain: Root Variance Frequency (RVF), Symbol Error Rate (SER), Entropy etc. Analyzing these features, we can identify and isolate a motor fault which is the foundation for the prognostics and health management of a system [9-12].

2. Modeling and Control of BLDC Motor

Unlike conventional DC Motor, rotor of the BLDC motor is a permanent magnet and the stator are coils working as electromagnets. Rotation of the permanent magnet (rotor) is achieved by controlling the magnetic fields generated by the electromagnets (stator). In practice, it is done by adjusting the currents into these electromagnet coils. Several studies have shown different control schemes for BLDC motors. D. Potnuru et. al. [13] proposed a closed loop control scheme, Sultan et. al. [14] discussed about sensor less control of BLDC motors based on experiments.

A conventional Generator-Motor (G-M) setup is chosen for BLDC motor diagnostic test to avoid complexity and ease in collecting data for non-stationary speeding and loading conditions. G-M setup allows us to build, control and modify the motor's external parameters efficiently. To perform tests on BLDC motor, the motor was coupled with a generator and some loads were connected to the generator. 9 The motor was controlled using a controller driver which has embedded Hall Effect Sensors (HES) and speed control potentiometer in it. Fig. 1 depicts the G-M setup diagram for the experiments.

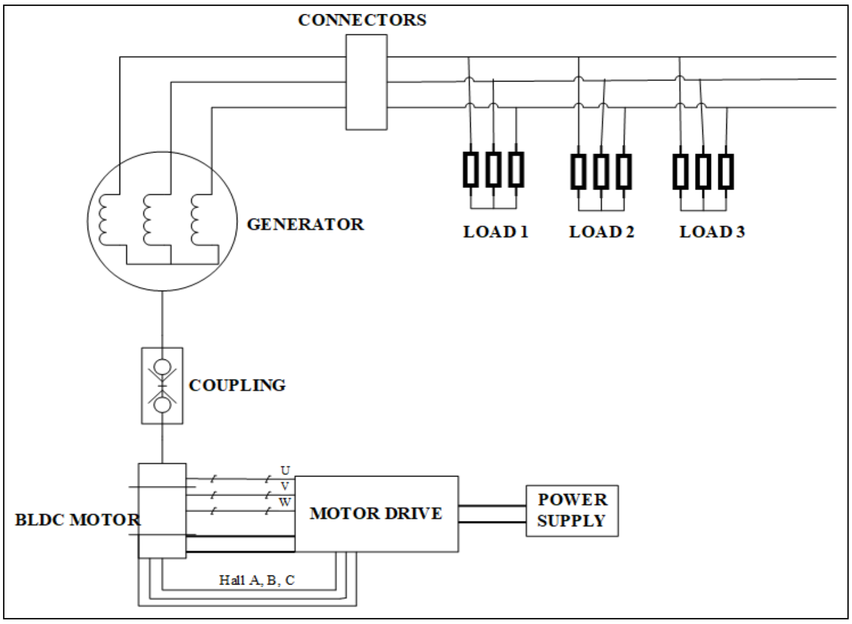

Fig. 1 - G-M set circuit diagram

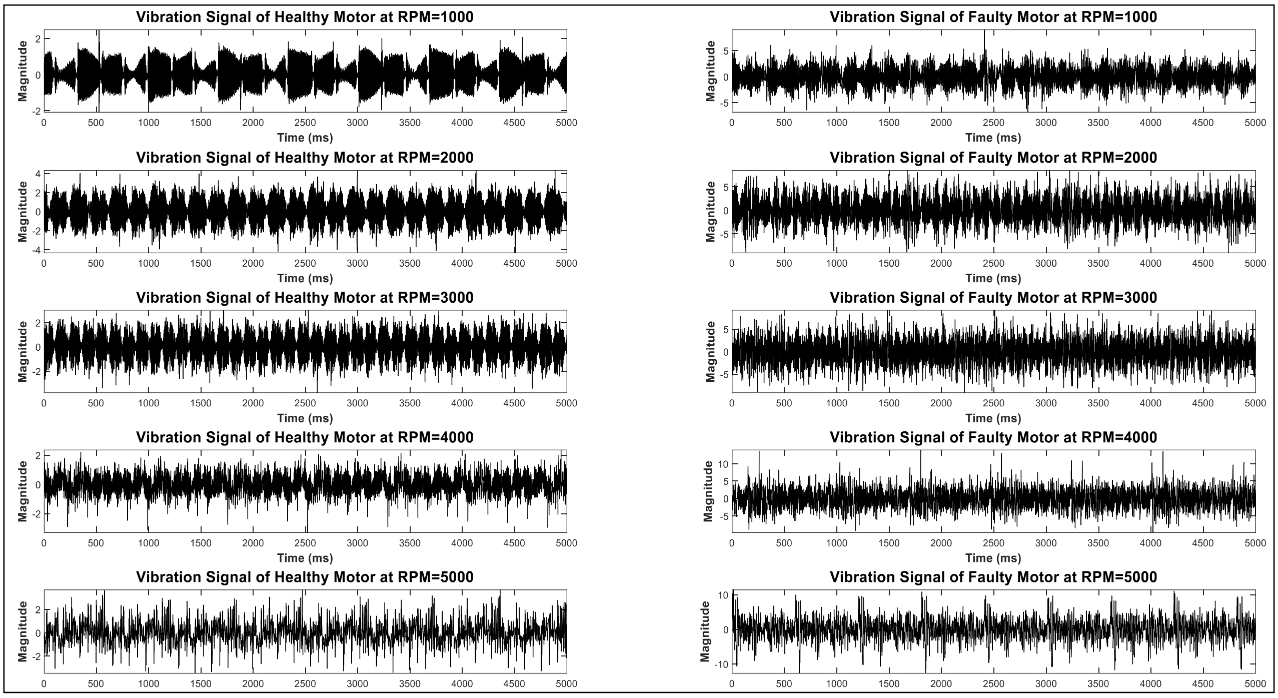

Fig. 2 - Vibration Signals at variable speeding conditions

3. Spectral Analysis

The motor was operated in variable speeding conditions from 500 to 5000rpm. Fig. 2 represents motor vibration signals in the time domain for both healthy and faulty cases. Although this representation does not give us adequate information to validate the fault state of motor, we can observe the state of signal visually and realize that for each speed of motor, faulty motor shows greater amplitude than the healthy one for same the time scale. Vibration samples were collected for a constant 30 kHz sampling rate and 5000 samples for each speeding condition were measured.

3.1 Discrete Fourier Transform (DFT)

To observe the frequency domain response, these uniformly spaced time samples (t), were transformed using Discrete Fourier Transform (DFT). Spectral analysis using Fourier transform is used to deconstruct the signal into its individual sine wave components. DFT allows us to speculate the frequencies and their proportions in original signal. Since each of the (t) contains a total of 5000 samples, calculating conventional DFT will be computationally too much expensive. An optimized FFT algorithm is used for the faster and efficient computation of DFT by taking advantage of symmetries in sine waves [15]. DFT for a time-domain signal (t) can be expressed as (1):

$$X_k = \sum_{n=0}^{N-1} x(t)\, e^{-\frac{i2\pi nk}{N}} \quad (1)$$

Where:

X_k = Transform Values

x(t) = Motor Vibration Signal

N = Number of Samples

k = Each k^{th} value is a complex number including amplitude and phase shift.

Fig. 3 illustrates the frequency response for vibration signals shown in Fig. 2. Analyzing the signals in frequency domain, clear fault sideband frequencies are observed. It is also noted that an increase in the motor speed causes the fault frequency magnitude to increase. At around 2 kHz frequency, no sideband is seen for healthy motor case for rpm 1000 to rpm 3000. However, a smaller sideband is observed for healthy state for rpm 4000 and rpm 5000 but that is quite smaller in magnitude compared to that of faulty state signal as shown in Fig. 2.

3.2 Short-time Fourier Transform (STFT)

DFT gives us only the frequency domain characteristics of a signal. In order to have time and frequency domain attributes of a non-stationary signal, we perform the Short-time Fourier Transform (STFT) of our signal. STFT allows us to portray the frequency content of a signal as a function of time [16, 17]. In STFT, the signal is truncated into narrow time intervals by selecting a window size. Later, Fourier transform is performed for consecutive segmented pieces where each Fourier transform then provides the spectral content of that time segment only. STFT can be defined as (2):

$$X(\tau, \omega) = \int_{-\infty}^{\infty} x(t)w(t-\tau)e^{-j\omega t}dt \qquad (2)$$

Where:

τ = Time Parameter

ω = Frequency Parameter

w = Window Function

Window function $(t-\tau)$ plays an important role on the outcome of STFT analysis. Wider analysis window gives us poor time resolution but good frequency resolution. On the other hand, narrow analysis window gives a good time resolution but a poor frequency resolution. So, before performing STFT, we have to choose an optimum window function and size by time-frequency trade-off. To perform STFT of BLDC motor vibration signal, Hann window with size 256 is chosen comparing the results to other window options.

Fig. 4 shows the spectrograms as STFT of motor vibration signals where the frequency is presented as a function of time. Observing the spectrograms, more regions with higher magnitudes are seen in faulty motor cases compared to the healthy as an evidence of signal's disorientation or fault. Spectrograms are presented as a heatmap representation of magnitudes.

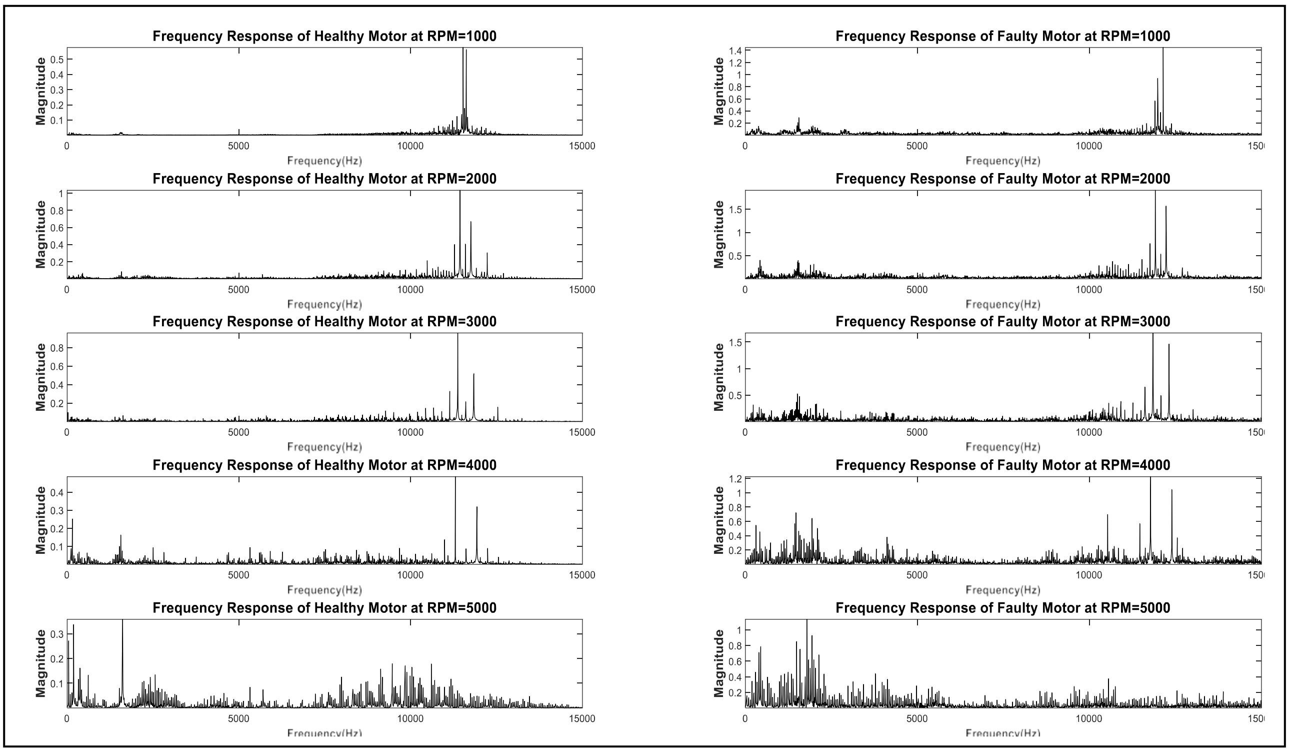

Fig 3 - Vibration spectrum comparison of motor vibration signals in frequency domain

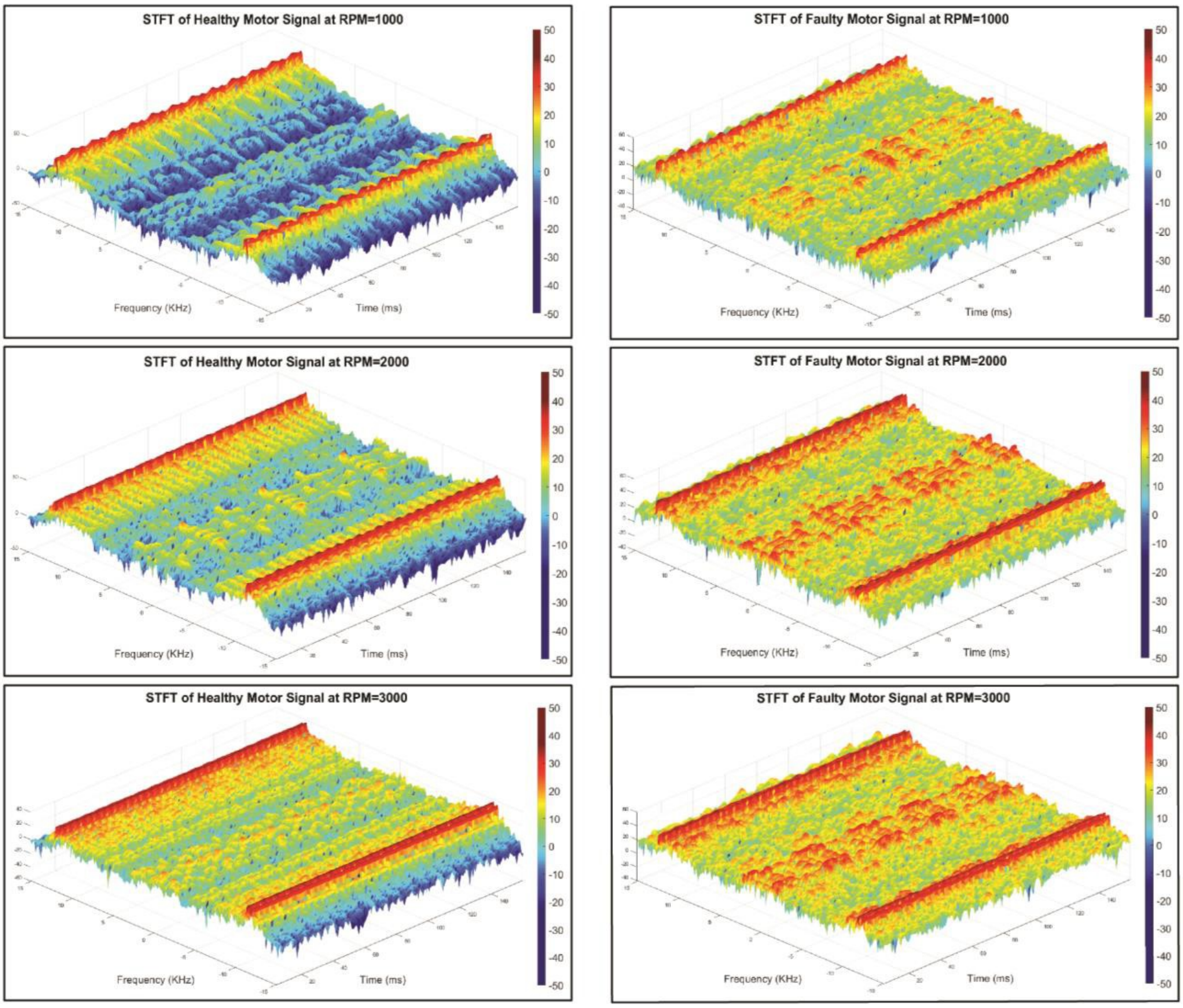

Fig. 4 - Time-Frequency analysis of vibration signals for different speeds

4. System Health Assessment

4.1 Condition Indicators

There are many CIs available for a system's condition assessment [18-22]. In this study, the most crucial ones are chosen for fault diagnosis that describe motor's condition best based on collected vibration samples. Below is the brief description of the features that are extracted from the time domain (1-7) and frequency domain (8-10) vibration signals.

1) Root Mean Square (RMS): RMS is a meaningful way of calculating the average of values over a period of time. RMS value is proportional to the power of the signal.

$$RMS = \sqrt{\frac{1}{N}\sum^{N}[x(n)]^2} \tag{3}$$

2) Variance: Variance is used to observe how individual signal components are related to each other for a given dataset. It takes in consideration all the deviations from the mean regardless of direction

$$Variance = \frac{1}{N-1}\sum_{n=1}^{N}[x(n)-\bar{x}]^2 \tag{4}$$

3) Kurtosis: It is a time domain feature that measures the thickness or heaviness of thetails of the signal by taking the bell curve as reference. A higher kurtosis value indicates signal contains of fault.

$$Kurtosis = \frac{N\sum_{n=1}^{N}[x(n)-\bar{x}]^4}{[\sum_{n=1}^{N}[x(n)-\bar{x}]^2]^2} \tag{5}$$

4) Skewness: Skewness means the degree of distortion from the normal distribution of signal data set. If the data are positively skewed, we can conclude that data have a long tail extending to the right of symmetric bell curve. Contrarywise, negatively skewed data have a long tail on the left.

$$Skewness = \frac{N\sum_{n=1}^{N}[x(n)-\bar{x}]^3}{[\sum_{n=1}^{N}[x(n)-\bar{x}]^2]^{3/2}} \tag{6}$$

5) Crest Factor: The crest factor of waveform is the ratio signal's peak value to its rms value. CF indicates how extreme the peaks are in a waveform.

$$Crest\ Factor\ (CF) = \frac{\frac{1}{2}\{\max[x(n)] - \min[x(n)]\}}{RMS} \tag{7}$$

6) Shape Factor: Shape Factor is a dimensionless number that characterizes the efficiency of the shape of a signal, regardless of its scale, for a given mode of loading.

$$Shape\ Factor\ (SF) = \frac{\sqrt{\frac{1}{N}\sum_{n=1}^{N}(x(n))^2}}{\frac{1}{N}\sum_{n=1}^{N}|x(n)|} \tag{8}$$

7) Impulse Factor: The ratio of peak value and the mean value of vibration samples is defined as the impulse factor.

$$Impulse\ Factor\ (IF) = \frac{\frac{1}{2}\{\max[x(n)] - \min[x(n)]\}}{\bar{x}} \tag{8}$$

8) Root Variance Frequency (RVF): RVF is the measurement of spectrum power convergence in the frequency domain. In (9), f_{char} stands for the characteristics frequency and f_s stands for the sampling frequency.

$$RVF = \sqrt{\frac{\sum_{n=1}^{N}(f_n - f_{char})^2 x(n)}{\sum_{n=1}^{N} x(n)}} \tag{9}$$

9) Symbol Error Rate (SER): It is the ratio of "number of samples in error" to the "number of transmitted samples".

$$SER = \frac{\sum_{n\in[f_{char}-f_s, f_{char}+f_s]} x(n)}{X_{char}} \tag{10}$$

10) Entropy: It is the measurement of system disorganization. Entropy provides a mathematical way to express the intuitive notion of signal's gradual disorder.

$$Entropy = -\sum_{n=1}^{N} \frac{x(n)}{\sum_{k=1}^{N} X_k} \log \frac{x(n)}{\sum_{k=1}^{N} X_k} \tag{11}$$

Calculating and analyzing these CIs, we can conclude on a system's state of health easily. Fig. 5 shows the comparison between different CIs and their trend of change for motor's healthy and faulty state vibration signals. From the graphs of different CIs at different operating conditions, we can observe that the RMS, Variance, Kurtosis, Skewness, CF, SF, SER and Entropy have higher values but RVF has a lower value at each operating condition.

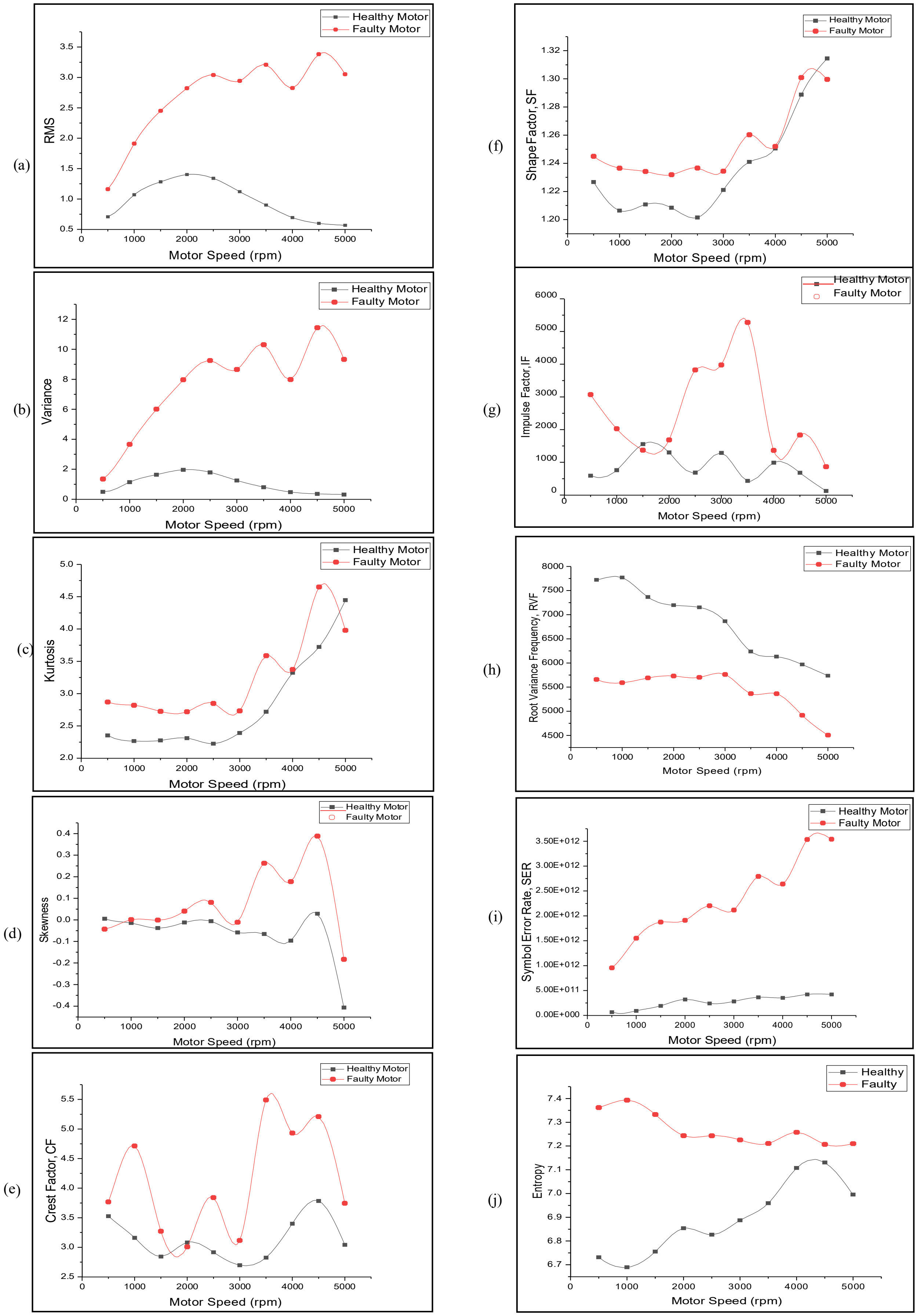

Fig. 5 - CI characteristics assessment for variable speeding conditions

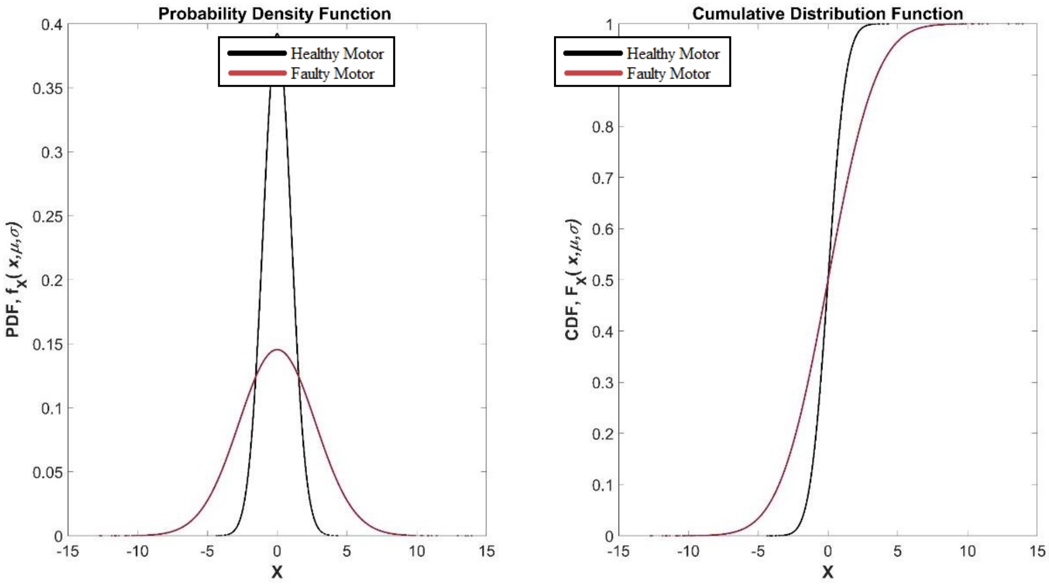

Fig 6 - (a) Normal PDFs for healthy and faulty motor; (b) Normal CDFs for healthy and faulty motor

4.2 Statistical Distributions

We took 25,000 vibration samples for healthy and faulty motor and illustrate the Probability Density Function (PDF) and Cumulative Density Function (CDF) as shown in Fig 6(a) and 6(b), respectively. PDF is defined as (12) and the relationship between PDF, $f_X(x)$ and CDF, $F_X(x)$ is: $f_X(x) = \frac{\partial}{\partial x}(F_X(x))$.

$$f_X(x|\mu,\sigma^2) = \frac{1}{\sqrt{2\pi\sigma^2}} e^{-\frac{(x-\mu)^2}{2\sigma^2}} \tag{12}$$

Probability distributions of a random data illustrate the probability in the sample space with mean (μ) and standard deviation (σ) of dataset. These distributions give us a better observation of mean and standard deviation of vibration samples [21-22]. From Fig. 6, the faulty state behavior of motor can be observed easily as the vibration signal is more dispersed in case of faulty motor.

5. Result Analysis and Discussions

In this study, several spectral analysis results for fault diagnosis are presented starting with Fourier transform. Fig. 3 illustrates DFT translations that carry clear evidence of fault frequencies at around 2 kHz frequency where abnormal fault sidebands are observed. The same vibration signals were analyzed in the time-frequency domain and spectrograms of STFT are plotted in Fig. 3. Spectrograms allow us to observe the signal in both time and frequency domain at the same time. A clear congruity indicating the faulty motor signals can be observed between FFT and STFT analysis for different operating conditions of the motor.

Condition Indicators described and plotted in Fig. 5(a)-5(j) carry out significant information for determining the SOH of a system. Higher values for CIs such as RMS, Variance, Skewness, Kurtosis, CF, SF, SER, Entropy indicate more disorientation and aberration of a signal. From Fig. 5(a)-5(f), 5(i), and 5(j) it can be observed that these CIs for the faulty motor signal show a higher value compared to the healthy motor signal in each operating condition. On the other hand, a lower RVF in Fig. 5(g) implies worse spectral power convergence in frequency domain for faulty motor signals. But there are some cases where similar results for both healthy and faulty cases are observed. Such as – Fig. 5(c) shows almost similar kurtosis values for healthy and faulty case at 4000 rpm, Fig. 5(d) shows lower skewness value for faulty state at 5000 rpm, Fig. 5(e) shows almost equal values of CF at 2000 rpm, Fig. 5(f) shows lower SF value at 5000 rpm for faulty case. Yet, observing the overall trend of CI and discrepancies between healthy and faulty state, it can be easily concluded that motor vibration signals in faulty state are much more disoriented compared to the healthy state. This dispersion can be further observed from the PDFs and CDFs of vibration samples illustrated in Fig 6. Amplitudes of vibration samples for healthy motor are distributed from -5 to +5 whereas for faulty motor it is around -10 to +10. Also, a wider distribution of faulty signal in Fig. 6(a) indicates a higher deviation from the mean of faulty signal compared to healthy signal.

Going through the overall analysis of spectrum, condition indicators, and probability distributions, we can conclude that there are certain anomalies between the vibration responses of the motor in healthy and faulty state. To speculate and isolate the fault condition, both the motors are dissembled and investigated as shown in Fig. 7. The faulty motor was passed

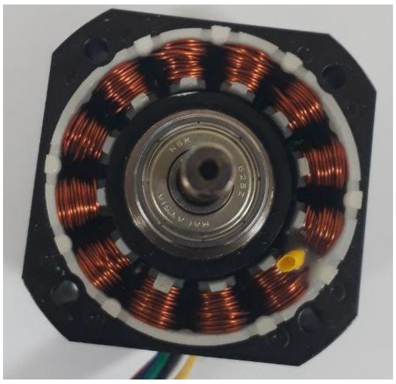
(a)

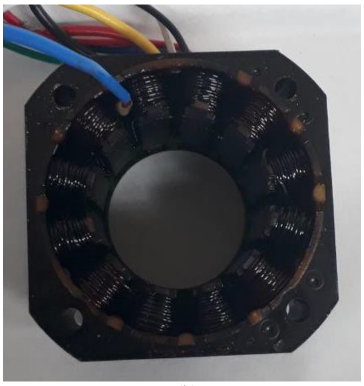
(b)

Fig. 7 - Stator coils in (a) Healthy state; (b) Faulty state

through several accelerated life tests with higher input and higher loading operations in order to acquire the fault state. Investigating the stator coils, it was found that several coils were burned and disconnected causing some short circuits in the stator windings. This wear out caused irregular excitations of stator coils and induced magnetic flux became unstable. Due to this irregular condition, the BLDC motor was showing some abrupt changes in its vibration.

6. Conclusions

This paper has reported the result analysis of BLDC motor tests under different operating conditions to isolate the faulty motor features from the healthy motor's through vibration signal analysis. Spectral analysis was done for frequency domain and time-frequency domain using different algorithms. Signal states in all domains are compared to distinguish and identify the anomalies in the motor vibration signal. Then, several condition indicators were extracted from the vibration signals that indicate the state-of-health of the system. Finally, some statistical distributions of the vibration samples are shown to illustrate motor's anomalous behavior graphically. All the approaches used have shown similar results although the process and algorithms were different for each approach. This gives a clear indication that there was a marginal change in the vibration of BLDC motor when the fault took place. Later, inspecting the stator coil, few wear out connections were found that was causing the short circuit in the stator winding.

Inspecting the signal changes of a system is the most essential attribute in system condition diagnosis. Fault diagnosis is the preliminary stage of system health monitoring that combines anomaly detection, fault isolation and prognostics of a system. Outcomes from this paper can be integrated with diverse industrial applications where BLDC motor is widely used and keep the system healthy as well as reduce the potential cost for repairing, maintenance etc.

Acknowledgement

This article is based on the results of a study carried out in support of Agency for Defense Development (RAM specialized laboratory, UD180018AD).

References

[1] Sang-Hoon Kim (2017). Electric Motor Control: DC, AC, and BLDC Motors. Elsevier Science, 389-416.

[2] Michael G. Pecht, Myeongsu Kang (2018). Prognostics and Health Management of Electronics: Fundamentals, Machine Learning, and the Internet of Things. John Wiley and Sons Ltd, 1-37.

[3] Jin, Xiaoning et al. (2016). Present Status and Future Growth of Advanced Maintenance Technology and Strategy in US Manufacturing. International journal of prognostics and health management. vol. 7, Spec Iss on Smart Manufacturing PHM (2016): 012.

[4] Chang-liang Xia (2012). Permanent Magnet Brushless DC Motor Drives and Controls. John Wiley and Sons Singapore Pte. Ltd, 1-62.

[5] Dongjin Lee & Rong Pan (2017). Predictive maintenance of complex system with multi-level reliability structure. International Journal of Production Research, 55:16, 4785-4801.

[6] David W. Coit, Enrico Zio (2018). The evolution of system reliability optimization, Reliability Engineering & System Safety. 106259.

[7] Boštjan Dolenc, Pavle Boškoski, Đani Juričić (2016). Distributed bearing fault diagnosis based on vibration analysis. Mechanical Systems and Signal Processing. Volumes 66–67, 521-532.

[8] Islam M.M.M., Islam M.R., Kim JM. (2017). A Hybrid Feature Selection Scheme Based on Local Compactness and Global Separability for Improving Roller Bearing Diagnostic Performance. In: Wagner M., Li X., Hendtlass T. (eds) Artificial Life and Computational Intelligence.

[9] Islam, M.M.M. & Kim (2017). Time–frequency envelope analysis-based sub-band selection and probabilistic support vector machines for multi-fault diagnosis of low-speed bearings. JM. J Ambient Intell Human Comput.

[10] Emmanue, O., Othman, M.L., Hizam, H., M. Othman, M., Aker, E., Chidiebere. A, O. and Samuel, T.N. 2019. Hybrid Signal Processing and Machine Learning Algorithm for Adaptive Fault Classification of Wind Farm Integrated Transmission Line Protection. International Journal of Integrated Engineering. 11, 4 (Sep. 2019).

[11] Moussa Hamadache, Joon Ha Jung, Jungho Park, Byeng D. Youn (2019). A comprehensive review of artificial intelligence-based approaches for rolling element bearing PHM: shallow and deep learning. JMST Adv. 2524-7913, 1-27.

[12] Chongqing Hu, Wade A. Smith, Robert B. Randall, Zhongxiao Peng (2016). Development of a gear vibration indicator and its application in gear wear monitoring. Mechanical Systems and Signal Processing. Volumes 76–77, 319-336.

[13] Devendra Potnuru, Alice Mary K., Saibabu Ch. (2018). Design and implementation methodology for rapid control prototyping of closed loop speed control for BLDC motor. Journal of Electrical Systems and Information Technology. Volume 5, Issue 1, 99-111.

[14] Sultan, N., Md Zain, B.A., Anuar, F.F., Yahya, M., Abdul Latif, I., Hat, M. and Al-alimi, S. 2019. Modeling and Speed Control for Sensorless DC Motor BLDC Based on Real Time Experiement. International Journal of Integrated Engineering. 11, 8, 55-64.

[15] Jinbao Yao, Baoping Tang, Jie Zhao (2016). Improved discrete Fourier transform algorithm for harmonic analysis of rotor system. Measurement. Volume 83, 57-71.

[16] R. Tao, Y. Li and Y. Wang (2010). Short-Time Fractional Fourier Transform and Its Applications. in IEEE Transactions on Signal Processing. vol. 58, no. 5, 2568-2580.

[17] Shujian Yu, Xinge You, Weihua Ou, Xiubao Jiang, Kexin Zhao, Ziqi Zhu, Yi Mou, Xinyi Zhao (2016). STFT-like time frequency representations of nonstationary signal with arbitrary sampling schemes. Neurocomputing. Volume 204, 211-221.

[18] Z. Gao, C. Cecati and S. X. Ding (2015). A Survey of Fault Diagnosis and Fault-Tolerant Techniques—Part I: Fault Diagnosis With Model-Based and Signal-Based Approaches. IEEE Transactions on Industrial Electronics. vol. 62, no. 6, 3757-3767.

[19] Robert Bond Randall (2011). Vibration-based Condition Monitoring: Industrial, Aerospace and Automotive Applications. John Wiley and Sons Ltd., 1-86.

[20] Byung C Jung, Jungho Park, Hyunseok Oh, Jisun Kim, Byeng D Youn (2015). A framework of model validation and virtual product qualification with limited experimental data based on statistical inference. Structural And Multidisciplinary Optimization, Volume 51, Issue 3, 573-583.

[21] Chao Hu, Byeng D Youn, Pingfeng Wang, (2019). Engineering Design Under Uncertainty and Health Prognostics. Springer International Publishing, 1-100.

[22] Sharma, V., & Parey, A. (2017). Gearbox fault diagnosis using RMS based probability density function and entropy measures for fluctuating speed conditions. Structural Health Monitoring. 16(6), 682–695.